Modeling of 4H–SiC multi-floating-junction Schottky barrier diode*

Pu Hong-Bin(蒲红斌), Cao Lin(曹 琳)†, Chen Zhi-Ming(陈治明),
Ren Jie(仁 杰), and Nan Ya-Gong(南雅公)

Department of Electronic Engineering, Xi'an University of Technology, Xi'an 710048, *China*

(Received 28 October 2009; revised manuscript received 19 January 2010)

This paper develops a new and easy to implement analytical model for the specific on-resistance and electric field distribution along the critical path for 4H–SiC multi-floating junction Schottky barrier diode. Considering the charge compensation effects by the multilayer of buried opposite doped regions, it improves the breakdown voltage a lot in comparison with conventional one with the same on-resistance. The forward resistance of the floating junction Schottky barrier diode consists of several components and the electric field can be understood with superposition concept, both are consistent with MEDICI simulation results. Moreover, device parameters are optimized and the analyses show that in comparison with one layer floating junction, multilayer of floating junction layer is an effective way to increase the device performance when specific resistance and the breakdown voltage are traded off. The results show that the specific resistance increases 3.2 $m\Omega\cdot cm^2$ and breakdown voltage increases 422 V with an additional floating junction for the given structure.

Keywords: silicon carbide, multi floating junction, Schottky barrier diode

PACC: 7110, 7340N, 7540B

1. Introduction

The purpose of designing power semiconductor devices is obtaining high breakdown voltage (V_R) while keeping the specific on-resistance (R_{on}) as low as possible. However, there is a tradeoff between breakdown voltage and specific on-resistance and its relationship was restricted by the theoretical silicon limitation.[1]

With silicon carbide (SiC) wafer localization and the maturing of high quality 6H–SiC and 4H–SiC epitaxial technology, SiC power devices have seen an upsurge in study. Generally, the SiC Schottky barrier is thinner than silicon at high voltages, and further improvement of SiC Schottky barrier blocking capability will be limited by reverse barrier tunneling leakage current. In order to take advantage of the SiC high critical breakdown field character, a pn junction and Schottky barrier composite structure (JBS or MPS) were proposed to eliminate tunneling current and achieve high blocking voltage. Further study of SiC Schottky barrier diode, minimum forward specific resistance without sacrificing blocking voltage could maximize forward current. So, the conventional design idea must be inadequate. During recent years, the super-junction (SJ) structure has been proposed and realized. For SJ Schottky barrier diode (SBD), 1000-V Si-based devices have been reported.[2] However, only the two research groups of Chow and Sheng had engaged in research of SiC SJ-SBD,[3,4] and they mainly focused on the structure simulation. The reason is that the charge must be strictly controlled in SJ devices,[5,6] otherwise breakdown voltage decreases rapidly. The other reason may be that it is very difficult to make deep implantation due to crystalline damage caused by the high energy implants, so there is no report about 4H–SiC SJ structure processing.

It is a hope to overcome these issues in the new structure, and consider the feasibility of the flow process, the floating junction (FJ)[7,8] structure with one floating junction layer used and optimized in our paper.[9] But the realization of high breakdown voltage becomes increasingly difficult due to the total compensation charge limited by one floating junction layer. Since, for 4H–SiC the control of activation rate of dopant into lattice is very difficult,[10] and it is very difficult to make high doping implantation due to crys-

*Project supported by the Open Fund of Key Laboratory of Wide Bandgap Semiconductor Materials and Devices, Ministry of Education of China.

†Corresponding author. E-mail: cl_zhifang@hotmail.com

© 2010 Chinese Physical Society and IOP Publishing Ltd

talline damage caused by the high energy implants. Two and more layers of junction may be a beneficial way to deal the problem.

The specific on-resistance and electric field distribution of the multilayer floating junction SBD along the critical path were analysed, employing a two-dimensional physically based device simulator MEDICI 4.0,[11] we have simulated the performance of FJ-SBD based on 4H–SiC. On-state resistance (R_{on}), electric field distribution and other character parameters were simulated, the device structure and the related parameter were discussed and optimized based on the results of analysis.

2. Device structure

The FJ structure features a floating p^+-buried layer embedded in the n^- drift region, as shown in Fig. 1. The drift region is divided into upper and lower sections by inserting FJ. With the p^+-buried floating layer, the depletion layer enhances development due to a mechanism similar to that of p-guard rings in planar terminations, when the depletion region from the Schottky contact reaches the p^+-buried floating layer, the voltage of the layer is pinned due to punch-through between the floating layer and the anode, and then a new depletion layer develops from the bottom of the p^+-floating layer toward the cathode. Compared with the conventional SBD form one triangle electric field, the FJ structures form two electric field distributions, and each triangular shape is formed at both upper and lower regions. Therefore, the FJ structures are used to provide the desired device performance with designing the peak field in the FJ below the critical field of 4H–SiC. So, the V_R of the device can be improved.

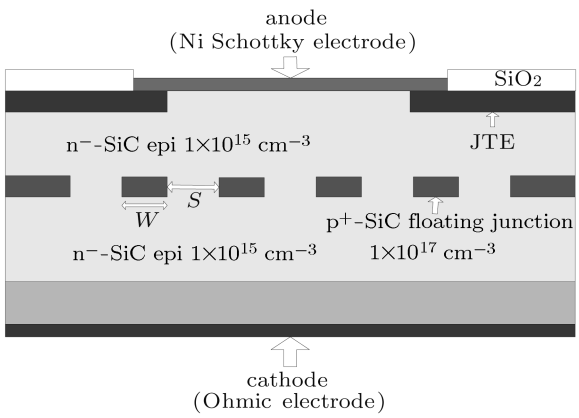


Fig. 1. Schematic drawing of FJ-SBD.

If we assume that the critical electric field is constant and the current path (narrowed by inserting the FJ) does not affect the R_{on}, then the V_R and R_{on} become n (number of drift regions) times larger than those of single drift region. In other words, R_{on} is proportional to V_R, rather than V_R^2 for the conventional structure. So, with the same voltage-sustaining layer, it is possible to increase doping concentration for lower R_{on} and therefore maintaining the same voltage blocking capacity.

There are two types of junction placement method for multi-floating junction, vertical and cross placement. Which one has priority will be discussed below.

3. Model for forward current conduction and electric field distribution

3.1. Forward current conduction

In FJ-SBD, the conductive channels in the drift region are separated into several parts, the basic forward conduction mechanisms of an FJ-SBD are the same as the conventional one except the resistance of the conduction channel through the adjacent junction which contributes to the most part of the resistance, so the width between adjacent junctions must be well designed in order to prohibit depletion layers pinch off conduct channel under zero and forward bias conditions. The specific resistances of the FJ structures are obtained based on the unit-cell structure as shown in Fig. 2.

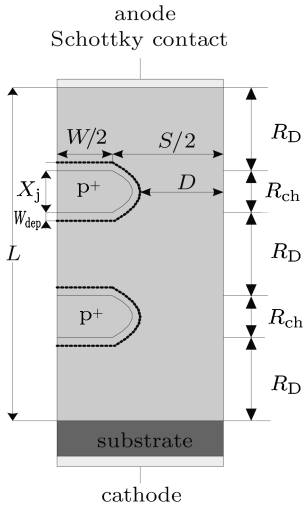


Fig. 2. Resistance composition in 4H–SiC FJ-SBD used for on-state analysis.

The p^+-type junction is formed by ion implantation through masked region of width S and open window of width W. For simplification of the calculation, the ion straggling in implantation and lateral diffusion after ion implantation were neglected.

The effective conduction width in the adjacent junction is related to the junction depletion width $W_{\rm dep}$

$$2D = S - 2W_{\rm dep}. \tag{1}$$

The doping concentration of the floating junction must be several times higher than the drift region, so the depletion width can be expressed as

$$W_{\rm dep} = \sqrt{\frac{2\varepsilon_0\varepsilon_{\rm r}(V_{\rm bi} - V_{\rm F})}{qN_{\rm D}}}, \tag{2}$$

where $\varepsilon_{\rm r}\varepsilon_0$ is the permittivity of 4H–SiC, $V_{\rm bi}$ is the p–n junction built-in voltage, and $V_{\rm F}$ is the forward biasing voltage.

No matter if it is vertical or cross placement, the specific on-resistance of the FJ-Schottky diode is determined by the resistance components as shown in Fig. 2, and can be expressed as

$$R_{\rm on} = (n+1)R_{\rm D} + nR_{\rm ch} + R_{\rm sub}, \tag{3}$$

where $R_{\rm ch}$ is the channel resistance, $R_{\rm D}$ is the drift region resistance, $R_{\rm sub}$ is the substrate resistance, and n is the number of the junction. The substrate is high doping, so the resistance can be neglected, the analytical expressions of $R_{\rm ch}$ and $R_{\rm D}$ are shown as

$$R_{\rm ch} = \frac{1}{q\mu_n N_{\rm D}} \cdot \frac{(X_j + 2W_{\rm dep})}{D} \cdot \frac{(W+S)}{2}, \tag{4}$$

$$R_{\rm D} = \frac{1}{q\mu_n N_{\rm D}} \cdot \frac{2(L - n\cdot X_j - 2n\cdot W_{\rm dep})}{n\cdot(W+S)}. \tag{5}$$

Assume that all the donor atoms in the drift region are ionized at room temperature. The model for the donor concentration dependence of the electron mobility[12] is as follows:

$$\mu_n(N) = 40 + \frac{950-40}{1+(\frac{N_{\rm D}}{2\times10^{17}})^{0.76}}\ {\rm cm}^2\cdot{\rm V}^{-1}\cdot{\rm S}^{-1}. \tag{6}$$

With this model, different component contributions of the specific resistances can be predicted.

The calculated results using our models are compared with MEDICI simulation results with the same structure parameters, as shown in Fig. 3. Our model achieves good agreement with the simulated results with different numbers of the junctions, the differences may be due to incomplete ionization, recombination, mobility with electric field and temperature, and other factors are not considered in our model.

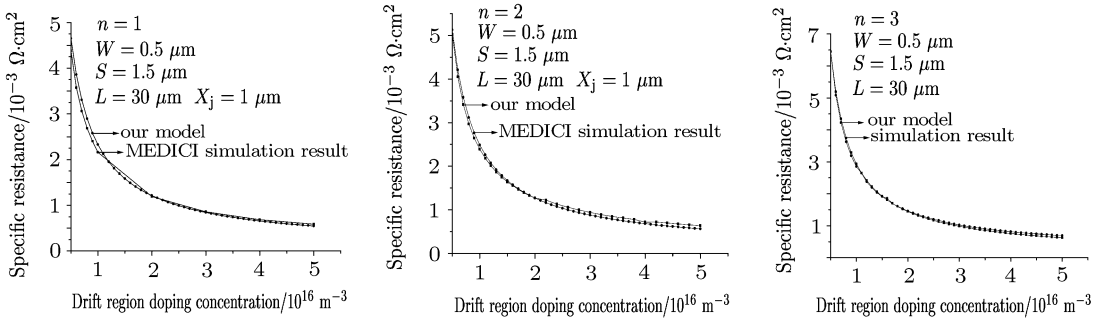


Fig. 3. Comparison of the calculated specific on-resistance using our model and the MEDICI simulation results at various doping conditions for different numbers of floating junction layer.

3.2. Reverse electric field distribution

Compared with conventional structures, we insert buried p^+-type FJ in the homogeneous drift region. When reverse voltage is increased, the electron and hole in the drift region and FJ were extracted by anode and cathode, whereas the immovable positive charge and negative charges remain at the instant of breakdown. In order to simplify the calculation, the electric field in the new structure is attributed to different types of charges with superposition concept,[8] the distribution in the middle of the junction is much larger than other position as shown in Fig. 4, which is called as critical path.

$$E = E_0 + E_{\rm n} + E_{\rm p}, \tag{7}$$

where E_0 is uniform field produced by applied voltage, which can be expressed as

$$E_0 = \frac{V_\mathrm{B}}{L}, \tag{8}$$

where V_B is the applied voltage, L is the drift region length, E_n is the electric field produced by positive charge in the drift region

$$E_\mathrm{n}(y) = \frac{qN_\mathrm{D}y}{\varepsilon_\mathrm{r}\varepsilon_0} = \frac{E_\mathrm{D}(L-2y)}{2L}, \quad E_\mathrm{D} = \frac{qN_\mathrm{D}L}{2\varepsilon_\mathrm{r}\varepsilon_0}, \tag{9}$$

where N_D is the uniform donor concentration in the drift region, E_D is the maximum value and other parameters have its conventional meaning. There are two types of plane-pattern of the p-buried layer for fabrication,[13] which are stripe pattern and dot pattern.

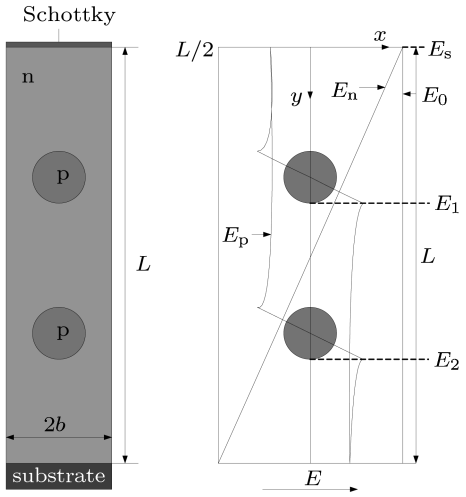


Fig. 4. Electric field profiles of E_0, E_n and E_p along $x = 0$.

For dot pattern, it is easy to calculate the electric field distribution with Gauss law as a charged ball, the electric field E_b can be expressed as:

$$E_{\mathrm{bd_i}} = \frac{N_\mathrm{A}qr}{3\varepsilon_0\varepsilon_\mathrm{r}} \quad (r \le R),$$
$$E_{\mathrm{bd_o}} = \frac{N_\mathrm{A}qR^3}{3\varepsilon_0\varepsilon_\mathrm{r}} \cdot \frac{1}{r^2} \quad (r > R). \tag{10}$$

For stripe pattern, assume that the length of the strip is infinite in comparison with the radius. By using Gauss law the electric field E_b distribution can be expressed as

$$E_{\mathrm{bs_i}} = \frac{N_\mathrm{A}qr}{2\varepsilon_0\varepsilon_\mathrm{r}} \quad (r \le R), \tag{11}$$

$$E_{\mathrm{bs_o}} = \frac{N_\mathrm{A}qR^2}{2\varepsilon_0\varepsilon_\mathrm{r}} \cdot \frac{1}{r} \quad (r > R), \tag{12}$$

where R is the radius of dot and stripe, r is the distance. It is difficult to consider the electric field distribution outside the junction because of the impact of other junction electric field distribution. For simplifying the calculation, we set the FJ layer as a uniformly charged infinite plane. The electric field is perpendicular to the plane and has nothing to do with distance,

$$E = \frac{\sigma}{2\varepsilon_\mathrm{r}\varepsilon_0}, \tag{13}$$

where σ is the surface charge density of the plane, for dot and stripe pattern, the electric field E_f can be expressed as

$$E_\mathrm{fd} = \frac{2\pi R^3 N_\mathrm{A}q}{3(W+S)^2\varepsilon_\mathrm{r}\varepsilon_0} \quad \text{(dot pattern)},$$
$$E_\mathrm{fs} = \frac{\pi R^2 N_\mathrm{A}q}{2(W+S)\varepsilon_\mathrm{r}\varepsilon_0} \quad \text{(stripe pattern)}. \tag{14}$$

The electric field reaches its maximum value at the Schottky contact and bottom of the junction along the central part of the junction as shown in Fig. 4. The electric field distribution can be expressed as

$$\begin{aligned}
E_\mathrm{s} &= E_0 + E_\mathrm{D} - nE_\mathrm{f},\\
E_1 &= E_0 + E_\mathrm{n}\left(y = \frac{L-2nR}{n+1} + 2R\right) + E_\mathrm{b} - (n-1)E_\mathrm{f},\\
E_2 &= E_0 + E_\mathrm{n}\left(y = 2\left(\frac{L-2nR}{n+1} + 2R\right)\right) + E_\mathrm{b} + (2-1)E_\mathrm{f} - (n-2)E_\mathrm{f},\\
E_z &= E_0 + E_\mathrm{n}\left(y = z\left(\frac{L-2nR}{n+1} + 2R\right)\right) + E_\mathrm{b} + (z-1)E_\mathrm{f} - (n-z)E_\mathrm{f},
\end{aligned} \tag{15}$$

where n is the total number of the FJ, z is the order of the junction counted from the top, E_z is the electric field under the z-th junction.

The electric field at the Schottky contact and the bottom of the junction with our model and MEDICI simulation when $n = 1$ is shown in Fig. 5, the difference between them is also illustrated. The difference becomes small when the reverse voltage increases, this accords with the above theoretical analysis.

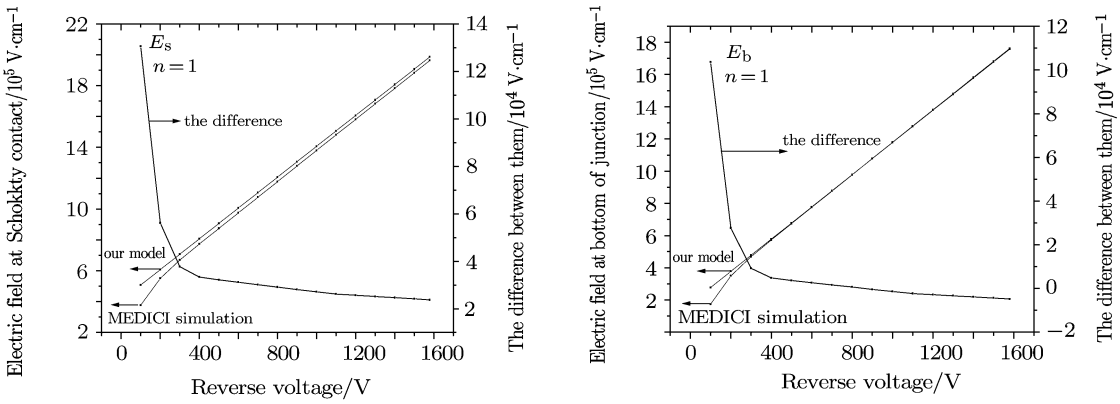


Fig. 5. Electric field calculated with our model in comparison with MEDICI simulation.

Figure 5 shows that the electric field reaches its maximum at the Schottky contact, the positive parts of the electric field is mainly determined by the applied voltage and the drift region doping concentration, the negative parts of the electric field is determined by the total doping in the floating junction when it looks as a uniformly charged infinite plane. In order to minimize the specific resistance, the drift region needs high doping and the junction does not pinch off under zero or forward bias, so the distance between two junctions must be large enough. For 4H–SiC, the doping concentration in the FJ was limited by flow process and cannot be too high, for the purpose of decreasing the electric filed at the Schottky contact, considering both the specific resistance and the flow process, together with two or more layers of FJ is the best way to increase the total doping of the floating junction for improving the device performance.

3.3. Optimization of FJ width and drift region doping concentration with one layer FJ

In order to simplify the calculation, the device will be broken down when the electric field exceeds the SiC critical breakdown field. The V_R reduces at smaller W. Because the field at the upper region deforms and increases the peak field with increasing S. The R_{on} rises at larger W, because the depletion region extended from the p^+n junction when the built-in potential pinches off the channel and hence the current does not flow. So there must be a trade-off between R_{on} and V_R, the simulation results show that they are balanced when $W = 0.4$ μm. When $W = 0.4$ μm, FJ doping of 1×17 cm^{-3}, the calculated results show that the specific resistance and drift region doping have an exponential relationship. There is a turning point when the drift region doping concentration is equal to 5×15 cm^{-3}. The breakdown voltage is a linear relationship with doping drift region. In order to guarantee lower forward on-resistance at the same breakdown voltage, we set doping drift region as 5×15 cm^{-3}.

3.4. The radius and doping concentration of the floating junction impact on the electric field of Schottky contact

Figure 4 shows that the negative parts of the electric field in the Schottky contact are contributed by the floating junction. The value of the electric field created by the FJ is mainly determined by the radius and doping concentration of the FJ, the relationship between them is shown in Fig. 6.

The electric fields created by the junction increase with the radius and doping, but limited by the forward resistance prohibit pinch off the channel. When we consider the feasible processing, adding more FJ layers may be a best way to deal with the problem.

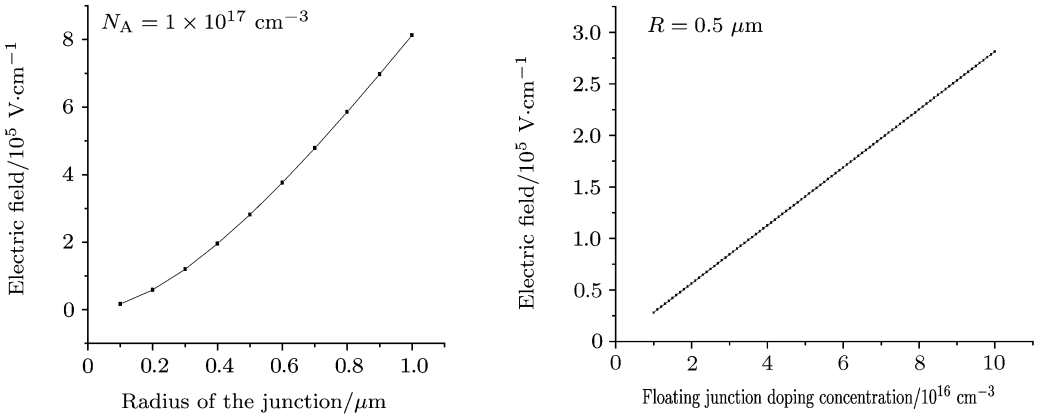


Fig. 6. Electric field at Schottky contact with different radius and doping concentration of the junction.

3.5. The number of FJ layers impact on the specific resistance and the breakdown voltage

Considering both the specific resistance and the breakdown voltage, we must need two or three or more layers of FJ, the influence of the number of the FJ on the R_{on} and V_R is illustrated in Fig. 7.

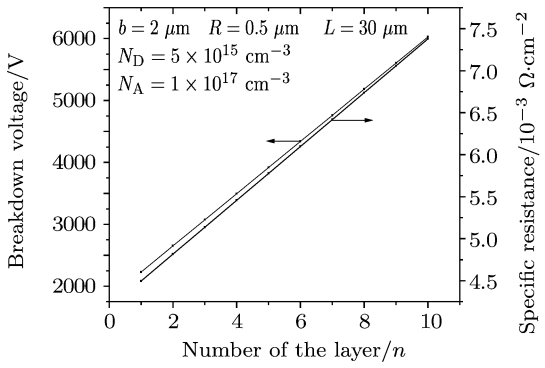


Fig. 7. Breakdown voltage and specific on-resistance with the number of the FJ layers.

The calculated results show that both R_{on} and V_R increase with the increase of junction layer, and both have linear relationship, the R_{on} increases 3.2 mΩ·cm^2 and V_R increases 422 V when an additional FJ is added.

4. Conclusion

An analytical model including both forward and reverse characters for multi-FJ-SBD is developed. The specific on-resistance was calculated and electric field distribution along the critical path was calculated with the concept of superposition, the result is in good agreement with the MEDICI simulation. In addition, the R_{on} and V_R of multi-FJ power SBDs were calculated and optimized with our model. The calculated results show that when the FJ width and spacing were 0.4 μm and 1.6 μm, drift region doping concentration is 5×15 cm^{-3}, its performance is excellent. The multi-FJ is a feasible way to increase the device performance in comparison with one FJ layer.

References

[1] Deboy G, Marz M, Stengl J P, Strack H, Tihanyi J and Weber H 1998 *Proc. IEDM 98* San Francisco, California, December, 1998 p. 683

[2] Napoli E and Strollo A G M 2001 *Proceedings of International Symposium on Power Semiconductor Devices and ICs*, Osaka, Japan, June 4–7, 2001 p. 339

[3] Chow T P, Zhu L and Losee P 2004 *International Journal of High Speed Electronics and Systems* **14** 865

[4] Sheng K and Yu L C 2008 *IEEE Trans. Electron Device* **55** 1961

[5] Adachi K, Johnson C M, Ohashi H, Shinohe T, Kinoshita T and Arai K 2001 *Mater. Sci. Forum.* **353** 719

[6] Tian B, Chen X and Kang B W 2006 *Microelectronics* **36** 1 (in Chinese)

[7] Cezac N, Morancho F and Rossel P 2000 *The 12th International Symposium on Power Semiconductor Devices and Ics* Toulouse, France, May 22–25, 2000 p. 69

[8] Chen X B, Wang X and Sin J K 2000 *IEEE Trans. Electron Devices* **47** 1280

[9] Pu H B, Cao L, Chen Z M and Ren J 2009 *J. Semicond.* **30** 40001

[10] Ikeda M, Matsunami H and Tanaka T 1980 *Phys. Rev.* B **22** 2842

[11] Palo A 1998 *MEDICI Two-Dimensional Device Simulation Programmer User Manual* (1st edn.) (Fremont: Avant) p. 1

[12] Roschke M and Schwierz F 2001 *IEEE Trans. Electron Devices* **48** 1442

[13] Wataru S and Ichiro O 2004 *IEEE Trans. Electron Device* **51** 797